

Nonlinear optical property of azo-dye doped liquid crystals determined by biphotonic Z-scan technique

Andy Ying-Guey. Fuh¹, Hui-Chi Lin², Ting-Shan Mo³, Ching-Hsu Chen²

¹Department of Physics and Institute of Electric-Optical Science and Engineering National Cheng Kung University, Taiwan, Taiwan 701, ROC

andyfuh@mail.ncku.edu.tw

²Department of Physics, National Cheng Kung University, Taiwan, Taiwan 701, ROC

³Department of Electronic Engineering, Kun Shan University of Technology, Taiwan, Taiwan 710, ROC

Abstract: This work investigates the optical Kerr property of azo-dye doped nematic liquid crystal films using the biphotonic Z-scan technique. The results indicate that the nonlinear effect measured using the Z-scan technique with a red light can be modulated or switched with the simultaneous application of a green light, because of photoisomerization and thermal effects, as determined by dynamic measurements. The former dominates in the early stage when the green light is applied, while the latter dominates in the later stage.

©2005 Optical Society of America

OCIS codes: (160.3710) Liquid crystals; (190.3270) Kerr effect.

References and links

1. I. C. Khoo, H. Li, and Y. Liang, "Observation of orientational photorefractive effects in nematic liquid crystals," *Opt. Lett.* **19**, 1723 (1994).
2. I. C. Khoo, "Orientational photorefractive effects in nematic liquid crystal films," *IEEE J. Quantum Electron.* **32**, 525 (1996).
3. M.-R. Lee, J.-R. Wang, C.-R. Lee, and A. Y.-G. Fuh, "Optically switchable biphotonic photorefractive effect in dye-doped liquid crystal films," *Appl. Phys. Lett.* **85**, 5822 (2004).
4. I. V. Tomov, T. E. Dutton, B. VanWanterghem and P. M. Rentzepis, "Temperature dependence of degenerate four wave mixing in azo dye doped polymer films," *J. Appl. Phys.* **70**, 36 (1991).
5. A. Y.-G. Fuh, C.-C. Liao, K.-C. Hsu and C.-L. Lu, "Laser-induced reorientation effect and ripple structure in dye-doped liquid-crystal films," *Opt. Lett.* **28**, 1179 (2003).
6. A. Y.-G. Fuh, C.-C. Liao, K.-C. Hsu, C.-L. Lu and C.-T. Tsai, "Dynamic studies of holographic gratings in dye-doped liquid-crystal films," *Opt. Lett.* **26**, 1767 (2001).
7. A. Y.-G. Fuh, C.-R. Lee and T.-S. Mo, "Polarization holographic grating based on azo-dye-doped polymer-ball-type polymer-dispersed liquid crystals," *J. Opt. Soc. Am. B* **19**, 2590 (2002).
8. C.-R. Lee, T.-S. Mo, K.-T. Cheng, T.-L. Fu and A. Y.-G. Fuh, "Electrically switchable and thermally erasable biphotonic holographic gratings in dye-doped liquid crystal films," *Appl. Phys. Lett.* **83**, 4285 (2003).
9. S. Slussarenko, O. Francescangeli and F. Simoni, "High resolution polarization gratings in liquid crystals," *Appl. Phys. Lett.* **71**, 3613 (1997).
10. M. Sheik-Bahae, A. A. Said, and E. W. Van Stryland, "High-sensitivity, single-beam n^2 measurements," *Opt. Lett.* **14**, 955 (1989).
11. M. Sheik-Bahae, A. A. Said, T. H. Wei, D. J. Hagan, and E. W. Van Stryland, "Sensitive measurement of optical nonlinearities using a signal beam," *IEEE J. Quantum Electron.* **26**, 760 (1990).
12. I. J'anossy and T. K'osa, "influence of anthraquinone dyes on optical reorientation of nematic liquid crystals," *Opt. Lett.* **17**, 1183 (1992).
13. T. K'osa and I. J'anossy, "Anomalous wavelength dependence of the dye-induced optical reorientation in nematic liquid crystals," *Opt. Lett.* **20**, 1230 (1995).
14. P. Palffy-Muhoray, H. J. Yuan, L. Li, and Michael A. Lee, "Measurements of third order optical nonlinearities of nematic liquid crystals," *Mol. Cryst. Liq. Cryst.* **207**, 291 (1991).
15. Andy Y.-G. Fuh, M.-S. Tsai, C.-R. Lee, and Y.-H. Fan, "Dynamical studies of gratings formed in polymer-dispersed liquid crystal films doped with a guest-host dye," *Phys. Rev. E* **62**, 003702 (2000).

16. Andy Y.-G. Fuh, M.-S. Tsai, L.-J. Huang, and T.-C. Liu, "Optically switchable gratings based on polymer-dispersed liquid crystal films doped with a guest-host dye," *Appl. Phys. Lett.* **74**, 2572 (1999).

Recently, the nonlinear effects of the azo-dye-doped liquid crystals (ADDLCs), such as the photorefractive effect¹⁻³ and degenerate four-wave mixing⁴, have recently attracted much interest. Khoo *et al.* was the first to report the photorefractive effect in ADDLCs^{1,2}. Intensity interference modulation induced by two coherent beams excites the azo-dye, and establishes a periodic distribution of space charges throughout the LC host. When a dc voltage is applied to the sample, the subsequent redistribution of the space charges induces a spatially inhomogeneous space-charge field, which periodically modulates the orientation of the LC molecules, resulting in a nonlocal refractive modulation in the cell. Such a nonlinear effect can be applied to holographic recording, phase conjugation, beam amplification, optical image processing, spatial filtering and others. Furthermore, ADDLCs have also been reported to be useful in fabricating holographic gratings (HGs), including intensity gratings^{5,6}, polarization gratings⁷⁻⁸ and biphotonic gratings⁹ using photoisomerization and photoinduced adsorption. This work reports the results obtained in an investigation of the nonlinear optical properties of ADDLCs, elucidated using biphotonic Z-scan technique. Z-scan¹⁰ is a simple, but powerful technique for measuring nonlinear refractive indices and nonlinear absorption coefficients. It has been applied to a wide range of materials, including liquid crystals¹¹⁻¹³. This investigation shows that the optical Kerr constant measured using the Z-scan technique with a red light can be modulated or switched by the simultaneous application of a green light, because of photoisomerization and thermal effects, according to the dynamic measurements. The former dominates in the early stage when the green light is applied, while the latter eventually dominates in later stage.

In this experiment, the nematic LC and the azo-dye were E7 (from Merck) and disperse red 1 (DR1) (from Aldrich). DR1 was doped into the LC host at a concentration of ~1wt%. The homogeneous mixture was injected into an empty cell, which was made from two indium-tin oxide (ITO)-coated pieces of glass separated by 25 μ m-thick spacers to form a sample. Each piece of ITO glass was treated with polyvinyl alcohol (PVA) and buffed to promote homogeneous alignment. The homogeneous alignment of the cell was firstly confirmed using a conoscopic technique.

Figure 1 presents the experimental setup. Light from a linearly polarized CW He-Ne laser ($\lambda=633$ nm), propagating in the z direction, was focused onto a narrow waist beam with a lens that has a focal length of 6.5 cm, producing a beam of radius ~11 μ m at the focus point. The intensity at the focus point was calculated to be $\sim 2.5 \times 10^6$ mW/cm². The sample was moved back or forth along the z axis near the beam waist of the He-Ne laser. When required, a linearly polarized CW diode-pump solid state (DPSS) laser ($\lambda=532$ nm) was simultaneously applied to the sample from its rear at an incident angle of ~5°. The green light was expanded so that it irradiated the sample as it moved. The He-Ne laser was polarized parallel to the DPSS laser. The far field transmitted intensity of the He-Ne beam was measured as a function of the sample position, using a photodetector placed behind a small iris. A neutral density filter (NDF), a color filter (CF) and a lens were installed in front of the photodetector to ensure that the photodetector received only red light. As the sample moved back or forth along the z axis near the beam waist, self-focusing or self-defocusing modifies the wavefront of the beam, and thereby changes the detected intensity of the beam. This setup was used to determine the nonlinear absorption coefficient β (from the curve of transmittance without an iris) and the optical Kerr coefficient n_2 . In this experiment, measurements were made at room temperature.

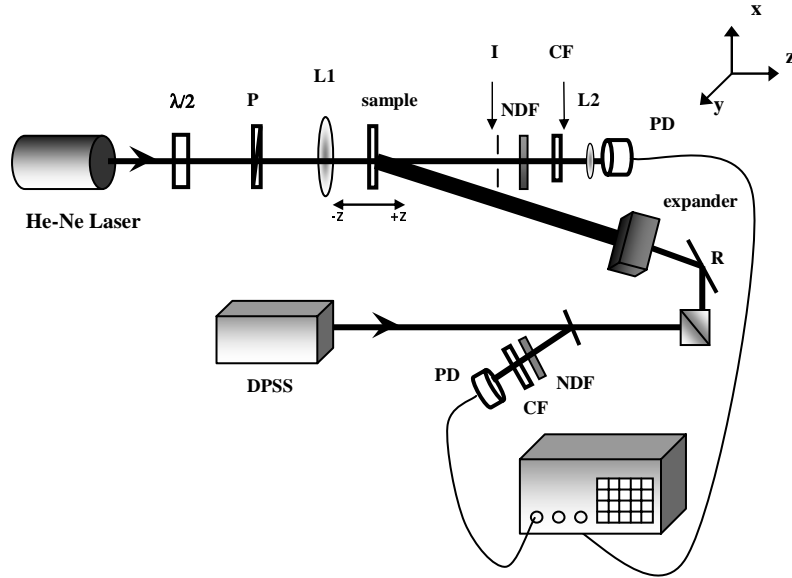


Fig. 1. Experimental set-up: P – polarizer; L – lens, I – iris; NDF – neutral density filter; CF – color filter; PBS – polarized beam splitter and PD – photodetector.

The nonlinear absorption coefficient was initially measured by Z-scan without an iris. The plotted Z-scan curve (not shown) was a straight line. It indicates that the nonlinear absorption coefficient β is zero, according to the following equation^{11,14}.

$$\Delta T_{abs} \cong -\frac{\beta}{2\sqrt{2}} I_0 (1-R) L_{eff}, \quad (1)$$

where ΔT_{abs} is the total change in transmittance as the sample is moved from a position far from the focus point to the focus point; R is the surface reflectivity, and $L_{eff}=(1-e^{-\alpha L})/\alpha$, where α and L are the linear absorption coefficient and the thickness of the sample, respectively. Figure 2 presents the measured biphotonic Z-scan results for azo-dye doped LC. Notably, the intensity at the focus of the He-Ne laser is fixed at 2.5×10^6 mW/cm², as the intensity of the green light (I_G) is varied. The curve in Fig. 2, without the application of a green light (diamond dots), shows the optical Kerr constant $n_2 \sim -1.74 \times 10^{-6}$ cm²W⁻¹. The nonlinear refractive index, n_2 , can be determined¹⁰⁻¹¹ from the peak-to-valley height (ΔT_{p-v}) of the diamond-dotted curve in Fig. 2, using the equation,

$$\Delta T_{p-v} \cong 0.406(1-S)^{0.25} \Delta \Phi_0, \quad (2)$$

where $S \sim 0.4$ is the linear transmittance of the iris and $\Delta \Phi_0$ is the phase distortion. The phase distortion is defined as $\Delta \Phi_0=2\pi L_{eff} \Delta n_0/\lambda$. The on-axis change in the index at the focus, Δn_0 , is linearly related to the nonlinear refractive index n_2 by

$$\Delta n_0 = n_2 I_0, \quad (3)$$

where I_0 is the intensity of the laser beam at the focal point. Equations (2) and (3) demonstrate that the nonlinear refractive index n_2 , obtained from the diamond-dot curve in Fig. 2, plotted based on a Z-scan, is -1.74×10^{-6} cm²W⁻¹. Similar experiments were performed in which the polarization of the He-Ne laser was perpendicular to the director axes in an azo-dye doped LC film and in pure LC (E7), to determine the origin of the value of n_2 obtained from the diamond curve in Fig. 2. The results show that the nonlinear refractive index n_2 of these two samples is zero. Therefore, the nonlinearity is believed to arise from the thermal effect induced by the

absorption of light by dye. In order to verify this result, the absorption spectra of the sample in the dark, and irradiated with a DPSS laser having an intensity $I_G \sim 124 \text{ mW/cm}^2$ for various times are measured and shown in Fig. 3. It can be seen from Fig. 3 that the absorption of the sample without the irradiation of the green beam is peaked at $\sim 567 \text{ nm}$. The absorptions at the wavelengths at the DPSS laser ($\lambda = 532 \text{ nm}$) and He-Ne laser ($\lambda = 632.8 \text{ nm}$) are 90%, 15% of the peak value, respectively. Thus, the He-Ne laser alone could induce the thermal nonlinear effect in the sample if its intensity is high enough. Generally, the azo dyes remain in the trans form in the dark. They absorb less light in the red region, as displayed in Fig. 3. After stimulating the sample with the green light, trans-isomers are photoisomerized to the cis form. The cis-isomers display new $n \rightarrow \pi^*$ type active transitions in the red regions. Since the laser is a Gaussian beam, the central region of the illuminated spot in the sample is hotter than the outer region. This difference between temperatures has a de-focusing effect. Figure 4(a) presents the temperature-dependent refractive index of a typical nematic LC, elucidating how the thermal effect causes defocusing. In the experiment, the polarization of the He-Ne laser was parallel to the LC director axis, so the central region of the illuminated spot had a smaller refractive index than the outer region, and n_2 was negative. Notably Fig. 2 shows that when a green light is applied simultaneously onto the sample, the Z-scan curve begins to vary. The peak-to-valley height ΔT_{p-v} initially increases with the intensity of the green light. The nonlinear refractive indices n_2 are measured to be $-1.76 \times 10^{-6} \text{ cm}^2 \text{ W}^{-1}$, $-2.61 \times 10^{-6} \text{ cm}^2 \text{ W}^{-1}$ and $-3.96 \times 10^{-6} \text{ cm}^2 \text{ W}^{-1}$ when I_G is set to 25, 68 and 98 mW/cm^2 , respectively. The I_0 in Eq. (3) for the calculation of n_2 coefficient in this biphotonic Z-scan is a sum of the intensities of He-Ne and DPSS laser beams. As I_G increases further ΔT_{p-v} decreases. Therefore, the variation in the nonlinear refractive index n_2 with additional irradiation with green light is believed to be caused by the thermal effect. The gradient of the temperature in the irradiated spot increases with the initial increase of the intensity of the green light (whose polarization is parallel to the LC direction). The thermal effect is more pronounced, and the difference between the refractive indices in the central and outer regions increases (Fig. 4(b)). The nonlinear refractive index n_2 becomes larger, as expected. The largest measured value of n_2 is $-3.96 \times 10^{-6} \text{ cm}^2 \text{ W}^{-1}$ when I_G is 98 mW/cm^2 . However, as the intensity of the green light increases further, the temperature of the whole illuminated spot approaches the clear temperature (T_C) of the sample, and the gradient of temperature in the irradiated spot decreases. The value of n_2 then decreases. When the green-beam intensity reaches a critical value, such that the temperature of the irradiated spot equals or exceeds T_C , the Z-scan curve becomes a horizontal straight line. (See the cross-dot curve in Fig. 2.)

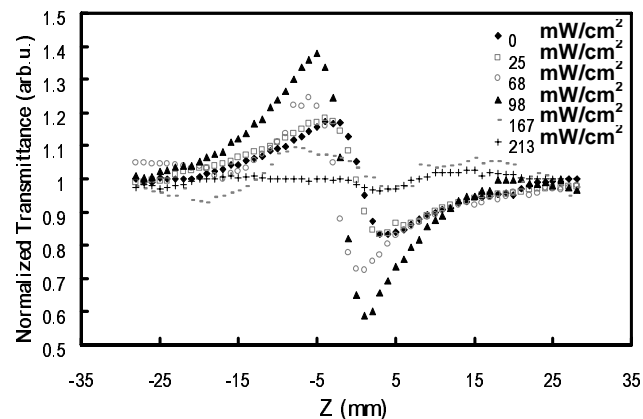


Fig. 2. Variations of the Z-scan transmittance in a nematic liquid crystal film doped with 1% azo-dye (DR1) with various intensities of green light. The curves are normalized with the transmittance measured at a point far behind the focus point.

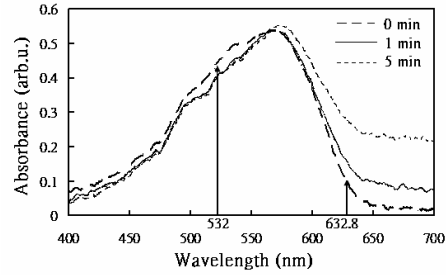


Fig. 3. The absorption spectra of the sample with the irradiation of a DPSS laser having an intensity of $\sim 124 \text{ mW/cm}^2$ for various times.

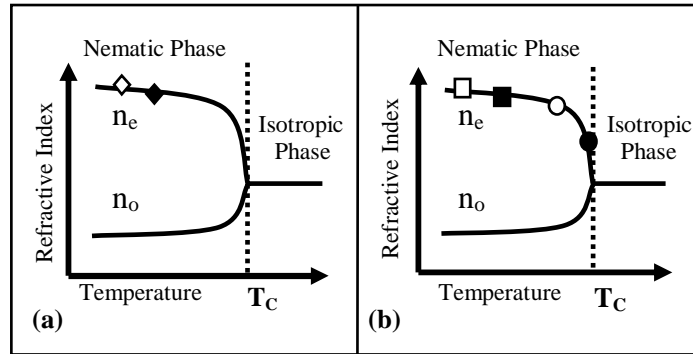


Fig. 4. Typical temperature-dependent refractive index of a nematic LC. (a) Diamonds plot temperatures of the sample without green light. (b) Squares and circles plot temperatures of the sample irradiated with green light with low and high intensities, respectively. Open and solid dots plot temperatures of the outer and central regions of the illuminated spot. T_C is the clear temperature of the LC.

The temperature variation of the sample with respect to the irradiating green laser intensity is measured. A digital K-type thermal couple thermometer was employed to measure the temperature variation. The result is shown in Fig. 5. It is clear to see from Fig. 5 that the temperature variation of the sample is proportional to the laser intensity. The transition temperature of E7 from the nematic to isotropic phase is $\sim 61^\circ\text{C}$. The result given in Fig. 5 is consistent with that in Fig. 2.

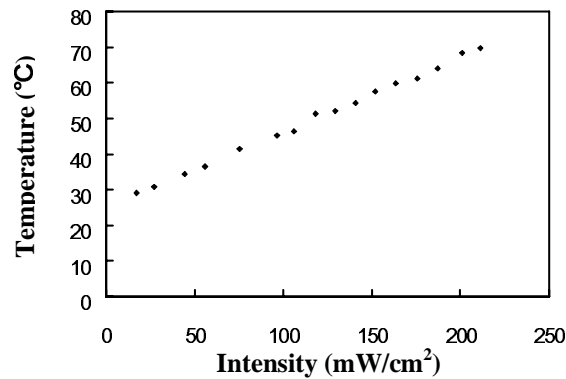


Fig. 5. Temperature variation of the sample with respect to the green light intensity.

The sample was turned such that the director axis of LCs (n) was perpendicular to the polarizations (P) of the He-Ne and the DPSS laser beams, to confirm that the thermal effect causes the nonlinear optical effect. No nonlinear effect was observed when only the red light was used. However, the self-focusing nonlinear effect was observed when a green light with an irradiance of $\sim 153 \text{ mW/cm}^2$ was applied. Figure 6 shows result. The polarizations of the laser beams are perpendicular to the director of the LCs, so the nonlinear refractive index becomes positive as expected. n_2 is measured to be $\sim 8.77 \times 10^{-7} \text{ cm}^2\text{W}^{-1}$. Notably, ΔT_{p-v} for the setup with $P//n$, in which no green light is applied, exceeds that with $P \perp n$ with $I_G \sim 153 \text{ mW/cm}^2$. This result is understandable, because the dichotic ratio of DR1 is positive.

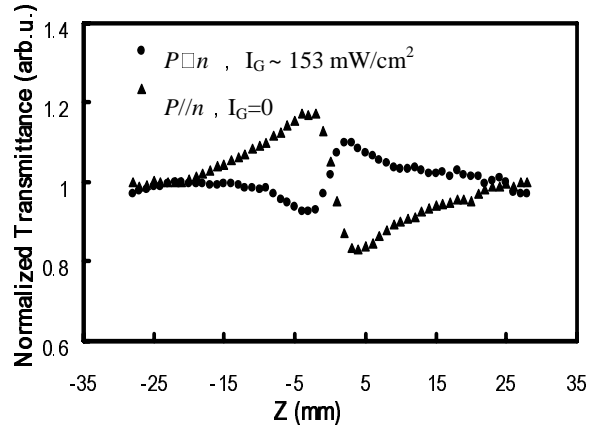


Fig. 6. Comparisons of Z-scan measurements made using the setup presented in Fig. 1 when the polarizations (P) of the He-Ne and DPSS lasers are perpendicular to the LC director (n) with those obtained with $P//n$ under $I_G=0$. Intensity of green light is 153 mW/cm^2 .

Figure 7 plots the dynamic Z-scan measurements when a green light is applied with $I_G=98 \text{ mW/cm}^2$. Curves (a) and (b) are the transmittances at the peak and valley points in the diamond-dot curve in Fig. 2 (without irradiation with green light), respectively. When the green light is turned on, the peak-to-valley height (ΔT_{p-v}) becomes smaller transiently, meaning that the transmittance at the peak point decreases, while the transmittance at the valley point increases. The cause is believed to be due to the photoisomerization effect as shown in Fig. 3. Before the green light is turned on, the refractive index at central region of the illuminated spot is smaller than that in the outer region. Immediately after the green light was turned on, the orientation of LCs is alerted. The green light induces the transformation by photoisomerization from the trans form to cis form, while the red light induces the inverse transformation by photoisomerization. The dye molecules follow the direction of liquid crystal molecules when dye molecules are in the trans form according to the guest-host effect¹⁵⁻¹⁶. When dye molecules are transformed to the cis form, they become orientated chaotically, and, in turn, reduce the order parameter of the liquid crystal. Based on the above reason, the guest-host effect is responsible for the fact that the change in the refractive index in the central region of the spot illuminated by the red-light (where the red light is strong) immediately after the green light is turned on is smaller than the corresponding change in the outer region (where the red light is weak). Thus, de-focusing effect is suppressed. At this time, n_2 decreases to $-1.39 \times 10^{-6} \text{ cm}^2\text{W}^{-1}$ from $-1.74 \times 10^{-6} \text{ cm}^2\text{W}^{-1}$. The I_0 used to calculate n_2 coefficient in Eq. (3) during such a transient period is I_R alone. In this transient period, I_G induces the transformation by photoisomerization from the trans form to cis form, while the I_R induces the inverse transformation by photoisomerization, and the resulted nonlinearly is Z-scanned using the red light. As the green light continues to be applied, the thermal effect

gradually strengthens, and eventually dominates. The peak-to-valley height (ΔT_{p-v}) increases. The results shown in Fig. 7 agree with those in Fig. 2. Finally, when the green light is switched off, ΔT_{p-v} decreases, and eventually returns to its original value. The transient response times of the transmittances at the valley position (curve (b) in Fig. 7) were also measured when green light pulses were applied ($I_G \sim 98 \text{ mW/cm}^2$). The valley transmittance was recorded as a pulse of green light ($I_G = 98 \text{ mW/cm}^2$) was applied for $\sim 330 \text{ ms}$. Figure 8 plots the results. The 10-90 % rise time is 40 ms and the 90-10 % decay time is 30 ms. The response time in the order of milliseconds is evidence of the molecular reorientation of LCs because of photoisomerization, which occurs transiently after a pulse of green light is applied.

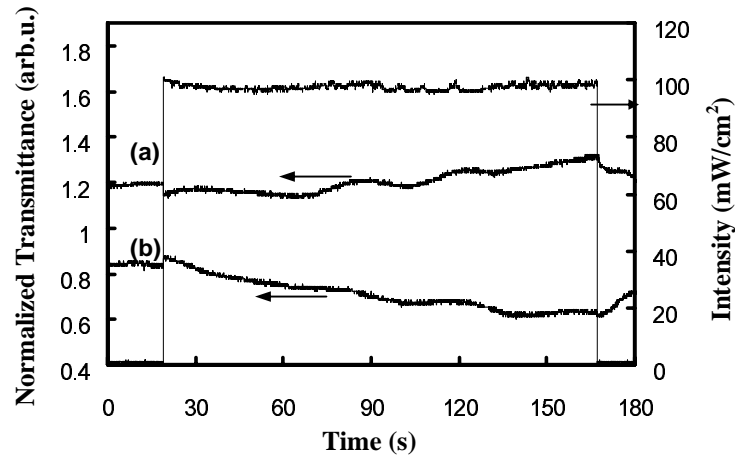


Fig. 7. Effects of dynamic Z-scan when green light is applied (98 mW/cm^2). Curves (a) and (b) are the transmittances at the two positions, at which the transmittances are maximal and minimal when no green light is applied.

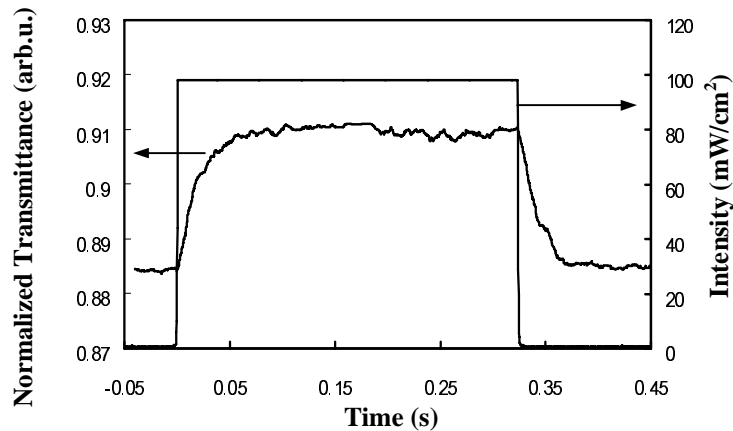


Fig. 8. Transient responses of the transmittances at the valley position (curve (b) in Fig. 7) when a pulse of green light is applied ($I_G \sim 98 \text{ mW/cm}^2$).

In conclusion, the biphotonic Z-scan effect in azo-dye doped LC films is demonstrated. The results demonstrate that the optical Kerr coefficient n_2 measured using Z-scan with a red beam can be modulated and/or switched by applying a green light laser. When green light is

simultaneously applied to the sample, the effect of photoisomerization (trans to cis) effect is observed transiently. The response times are ~30 - 40 ms.

The authors would like to thank the National Science Council (NSC) of the Republic of China (Taiwan) for financially supporting this research under Contract No. NSC 93-2112-M-006-016.